Optimal Residential Demand Response for Multiple Heterogeneous Homes With Real-Time Price Prediction in a Multiagent Framework

Zhanle Wang, *Student Member, IEEE*, and Raman Paranjape, *Member, IEEE*

***Abstract*—Demand response (DR) is a recent effort to improve the efficiency of the electricity market and the stability of the power system. A successful implementation relies on both appropriate policy design and enabling technology. This paper presents a multiagent system to evaluate optimal residential DR implementation in a distribution network, in which the main stakeholders are modeled by heterogeneous home agents (HAs) and a retailer agent (RA). The HA is able to predict and control electricity load demand. A real-time price prediction model is developed for the HA and the RA. The optimal control of electricity consumption is formulated into a convex programming problem to minimize electricity payment and waiting time under real-time pricing. Simulation results show that the peak-to-average power ratio and electricity payments are significantly reduced using the proposed algorithms. The HA, with the proposed optimal control algorithms, can be embedded into a home energy management system to make intelligent decisions on behalf of homeowners responding to DR policies. The proposed agent system can be utilized to evaluate various strategies and emerging technologies that enable the implementation of DR.**

***Index Terms*—Convex optimization, electric vehicle (EV), multiagent system (MAS), real-time pricing (RTP), residential demand response (DR).**

NOMENCLATURE

Sets

$\mathcal{AC}$	Set of actions.
$\mathcal{AG}$	Set of agents.
$\mathcal{AP}$	Set of appliances in a home.
$\mathcal{BAP}$	Set of background appliances.
$\mathcal{CAP}$	Set of controllable appliances.
$\mathcal{E}$	Set of environment characteristics.
$\mathcal{GA}$	Set of generator agents (GAs).
$\mathcal{HA}$	Set of home agents (HAs).
$\mathcal{RA}$	Set of retailer agents (RAs).
$\mathcal{RS}$	Retailer service scope set.
$\mathcal{T}$	Time horizon set.

Variables and functions

α_1, α_2	Slopes in the price prediction model.
β_1, β_2	Constants in the price prediction model.
λ^{ap}	Dissatisfaction factor of scheduling appliance ap.
Δt_{total}	Time to charge up an electric vehicle (EV) from zero state of charge (SOC).
Δt^{ap}	Cycle length of operating appliance ap.
ap	Appliance.
ct	Constraint.
$\widehat{E_B^{\text{ap}}}$	Predicted electricity energy of background loads (column vector).
$\widehat{E_C^{\text{ap}}}$	Predicted electricity energy of controllable loads (column vector).
L	Column vector of load.
$\hat{L}$	Column vector of predicted load.
l_t^{ap}	Electricity load of appliance ap at time t.
$\widehat{l_t^{\text{ap}}}$	Predicted electricity load of ap at t.
l_{TH}	Load threshold in the price prediction model.
$\text{occ}(t)$	Number of active occupants at t.
P	Column vector of electricity price.
p_t	Electricity price at time t.
$p(\cdot)$	Price based on load.
$\text{pr}(t\|\text{ap})$	Probability of using an appliance ap $\in \mathcal{AP}\backslash\text{EV}$ at t.
$q_{\text{rated}}^{\text{ap}}$	Rated power of the appliance ap.
soc_0	Initial SOC.
t	Time slot.
t_0^{ap}	Time of starting to operate an appliance ap.
t_1^{ap}	Time when operation of the appliance must complete.
w^{ap}	Waiting time vector of an appliance ap.

Manuscript received March 19, 2015; revised May 25, 2015, July 7, 2015, and September 1, 2015; accepted September 8, 2015. Date of publication October 8, 2015; date of current version April 19, 2017. This work was supported by SaskPower, a provincial utility in Saskatchewan, Canada. Paper no. TSG-00325-2015.

The authors are with Electronic Systems Engineering, University of Regina, Regina, SK S4S 0A2, Canada (e-mail: zhanle.wang@gmail.com; raman.paranjape@uregina.ca).

Color versions of one or more of the figures in this paper are available online at http://ieeexplore.ieee.org.

Digital Object Identifier 10.1109/TSG.2015.2479557

I. INTRODUCTION

DEMAND response (DR) is designed to reduce peak demand and encourage electricity consumption when renewable energy is available in response to market price and/or power availability over time [1], [2]. It provides a variety of financial and operational benefits to electricity customers, load-serving entities, and grid operators [2], [3].

Power generation is always required to match the time fluctuated load as electricity cannot be stored economically. Furthermore, the dispatch of power generation units is primarily based on generation cost. Consequently, electricity generation costs are generally proportional to the amount of

the load. However, this fluctuating generation cost or the wholesale electricity price due to multiple generators is mostly hidden by the retailer/utility with a flat electricity tariff for the user. Price-based DR programs can reveal the actual electricity price to encourage end users to change consumption patterns and shift electricity demand from peak demand periods to off-demand periods in order to improve energy efficiency. The U.S. Department of Energy lists three types of price-based DR options: 1) time-of-use; 2) real-time pricing (RTP); and 3) critical peak pricing [3]. Another type of dynamic tariff is inclining block rate (IBR), in which the electricity price is higher when the energy consumption exceed a certain threshold over a period of time, e.g., stepped residential rates used by BC Hydro (BH) [4].

Besides the incentive mechanisms, a successful DR implementation also relies on DR enabling technologies since it is very difficult (if not impossible) for consumers to track dynamic pricing. In a residential sector, DR enabling technologies are available in the context of a smart home. The smart home features an energy management system (EMS) that intelligently controls household loads through an association between smart meters, smart appliances, EVs, small home power generation and storage, etc. [5].

Developing efficient DR models to evaluate the effectiveness of DR policies and enabling technology are vital to an implementation of a DR program aiming to improve energy efficiency and power system stability. There is a trend that the smart grid moves toward to a distributed system with a large number of heterogeneous components [6]. An efficient residential DR model should implement heterogeneous residential load forecasting, multicriteria optimization (e.g., objectives for individual homes, utilities, and aggregations of them) and intelligent distributed algorithms to evaluate the complex and large-scale power systems.

An effective real-time load forecasting model is crucial for a utility to adjust its generation and to provide a baseline for evaluating DR. Previous reviews of residential electricity load prediction models identify two main types of simulation models: 1) top-down; and 2) bottom-up [7], [8]. A physical-based DR-enabled aggregating residential load is presented in [9]. Individual controllable load models are also studied, e.g., air conditioning [10] and water heaters [11].

A variety of researchers have modeled residential DR as an optimization problem under RTP. The main purpose of these studies is to develop optimization mechanisms for minimizing residential customers' electricity payment [12]–[17] or maximizing their utilities/welfare in order to achieve a generally uniform electricity load profile with a reduced peak-to-average power ratio (PAPR) [18]–[20]. In [12], a single home optimal residential DR is formulated to a linear programming (LP) problem to minimize electricity payment and waiting time under RTP. DR implementation considering a single home operating different appliances is modeled using a convex programming (CP) to minimize electricity payment in [13]. Furthermore, this paper also introduces 1-norm regularization to deal with binary decision variables. A optimization model is also proposed in a scenario of multiple houses to maximize users' utilities in [20]. A coordinated DR scheme with a distributed algorithm is proposed in [21] and [22] to avoid new peak demand due to customers' response to lower prices. In addition to the optimality of electricity expense or social welfare, the study in [23] also evaluates the fairness. A comprehensive view of optimization algorithms for DR applications can be found in [24].

A multiagent system (MAS) generally refers to a body of multiple autonomous agents that interact, cooperate, and negotiate with each other in order to satisfy their designed objectives [25]. A comprehensive review from the IEEE Power Engineering Society's Multi-Agent Systems Working Group identifies that an MAS can provide two novel approaches for power engineering: 1) building flexible and extensible systems and 2) simulation and modeling [26]. MAS is particularly suitable for modeling heterogeneous components in the DR application for the smart grid.

The research literature includes a wide range of work using MAS to evaluate DR implementations. DR program incorporating with distributed energy resources (DERs) and distributed storage is evaluated in [27] using an index-based incentive mechanism. The study in [28] proposes a ecosystem to optimize DR implementation and DER management in a residential sector using hierarchical agents. Agent-based systems are also proposed to associate DER and storage facilities with DR in order to reduce peak demand and minimize electricity payment [29]. The study in [22] proposes an MAS to solve a bi-level optimization problem using a iterative distributed algorithm to avoid peak rebounds in lower price periods and to achieve a flatten total load profile. An agent-based model is developed to evaluate the home EMS in residential DR implementation [30]. MAS can also be found in applications for coordination of EV charging [31], [32] and microgrids control [33]–[35].

Game theory as a mathematical model of interaction, competition, and cooperation among self-interested agents [36] is widely applied to study DR. The study in [37] presents a two-stage (Stackelberg game in the first stage) two-level model for a smart grid retailer as an intermediary agent considering both DR for consumers and market price uncertainty. The model is reformulated to a mixed-integer LP problem. The dynamic prices in [38] for a DR application are determined by a game, in which an RA and a customer agent are players. The RA minimizes the electricity payment using LP while the customer agent maximizes its daily profit. Although the game theory applications for DR in [39] and [40] do not use agent systems, the players in the games can be naturally modeled by autonomous agents.

In this paper, we consider RTP as the DR policy since it reveals wholesale electricity prices and provides the most precise way among others to schedule household load. We propose an MAS for modeling optimal residential DR, in which the main stakeholders are modeled by HAs and an RA. A heterogeneous residential load prediction model, a price prediction model, and a load control model are also developed, which are incorporated to the HAs. The primary purpose is to evaluate the two key components of a DR program, namely DR policies and enabling technologies. The DR policy that this paper focuses on is RTP; however, the proposed model can

be readily extended to incorporate other strategies, e.g., direct load control (DLC). The second purposed is to develop an optimal distributed control algorithm for scheduling heterogeneous household electricity usage to improve energy efficiency. The optimal scheduling/controlling task is formulated to a CP problem.

In general, the differences between this paper and the studies in the literature include the following.

1) The HAs in this paper are heterogeneous with unique individual load profiles forecasted by a residential load prediction model. This prediction model forecasts household load including EV charging based on statistical information of how people operate their appliances.
2) The HAs minimize electricity payment and waiting time using local load information and predicted electricity price to schedule controllable load/appliances; therefore, the communication among homes is at a minimum level and the privacy of information is protected.
3) Since the proposed mechanism is a distributed algorithm and it does not require communication among homes, the method is linearly scalable and can be implemented in parallel into a very large system.
4) We evaluate both the benefits for individual HAs and aggregated benefit for the RA daily.

The study in [12] defines RTP as a function of energy and evaluates DR for a single home over a period of four months. The RTP in this paper is defined as a function of power. We have shown a reduction of the electricity payment, the peak demand, and the PAPR on a daily basis. Scheduled daily electricity usage plays a significant role in DR implementations since having a more uniform daily load profile is more beneficial than scheduling loads over different days. In [13], electricity allocation of various appliances under RTP is evaluated; however, the aggregated load of multiple appliances and the electricity payment saving is not provided. To avoid new peak demand due to customers' response to low prices, the work in [21] and [22] proposes coordinated DR schemes. Our approach is to provide HAs the ability to predict electricity prices instead of requiring intensive communication.

The contributions of this paper are summarized as follows.

1) We propose an MAS to evaluate benefits from DR for heterogeneous multiple HAs associated with a residential load prediction model. This model forecasts the baseline for household electricity usage including EV, which is based on statistical probability information of how people use their appliances.
2) We develop an optimal load control model for HAs to schedule electricity usage to observe both the individual benefit for an HA and the aggregated benefits for an RA from DR. Each HA minimizes its electricity payment and waiting time to find a tradeoff based on its heterogeneous local information. Furthermore, the benefits of DR are emphasized from comparing with the predicted reference.
3) The proposed mechanism does not require coordination between HAs; therefore, it only requires a minimum of communication between the utility/retailer and multiple homes. This is greatly useful because the infrastructure for communication is still under development. Since HAs minimize electricity payments locally due to the proposed price prediction model, the privacy of users is not sacrificed.
4) Since the residential load prediction model is based on statistical information, with tailoring the probabilities of using appliances to a specific area/city, the proposed MAS can be a test bed to evaluate various DR policies and enabling technologies.

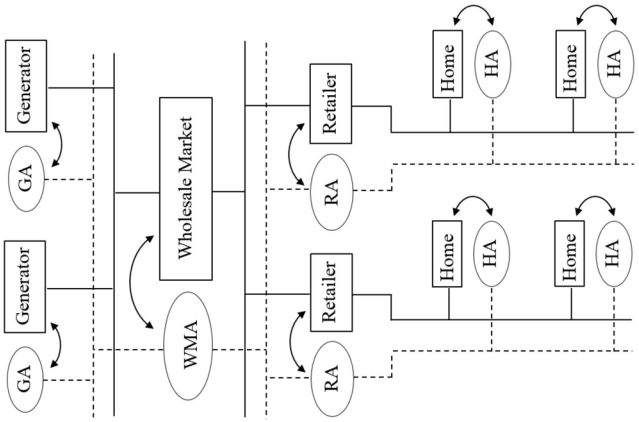

Fig. 1. MAS architecture (the solid line represents power line and the dash line refers to LAN).

The rest of this paper is organized as follows. The MAS design is illustrated in Section II. Section III discusses the mechanism to predict electricity prices and the models to predict and control the household load. Simulation results are shown in Section IV. A discussion of this paper is presented in Section V followed by the conclusions.

II. Multiagent System Design

This paper considers a general electricity wholesale market. Similar to other commodities, electricity can be traded in wholesale markets and retail markets. In general, retailers/utilities can purchase electricity from a wholesale market and sell it to customers in a retail market [41]. Retailers/utilities may also own generators and sell electricity directly to end users. We use the umbrella term of purchase to denote buying power from a wholesale market and/or generating power. This does not lose generality since the electricity price could be considered as generation cost if the retailer/utility generates power.

This general wholesale electricity market scenario is modeled by an MAS shown in Fig. 1, in which each component is captured by a corresponding agent: wholesale market agent (WMA), RA, HA, and GA. The agents are connected by a local area network (LAN) or the Internet. Although all the agents are defined, we only focus on the power and information flow in the distribution network from a retailer/utility to end users/homes. However, this paper can be readily extended to other aspects of the power system.

Following the abstract architecture for agents in [25], the proposed MAS has a set of agents as follows:

$$\mathcal{HA} = \{HA_1, HA_2 \ldots\} \tag{1}$$

$$\mathcal{RA} = \{RA_1, RA_2 \ldots\} \tag{2}$$

$$\mathcal{GA} = \{GA_1, GA_2 \ldots\} \tag{3}$$

$$\mathcal{AG} = \mathcal{HA} \cup \mathcal{RA} \cup \mathcal{GA} \cup \text{WMA} \tag{4}$$

where $\mathcal{HA}$ and $\mathcal{RA}$ are the set of HAs and RAs, respectively. The union of these agents forms the multiagent set $\mathcal{AG}$. We also define a retailer scope set $\mathcal{RS}$

$$\mathcal{RS} = \{RA, HA_1, HA_2, \ldots\} \tag{5}$$

which contains an RA itself and all the HAs whom the RA delivers electricity to.

All agents perceive their environment, which is characterized by a set $\mathcal{E}$

$$\mathcal{E} = \{e_1, e_2, \ldots\}. \tag{6}$$

Autonomous agents are capable of perceiving their environment, upon which they take actions. Let $\mathcal{AC}$ denotes the set of actions

$$\mathcal{AC} = \{a_1, a_2, \ldots\}. \tag{7}$$

Time t is discretized into time slots. Let $\mathcal{T}$ denotes the set of time slots in sequence

$$\mathcal{T} = \{1, \ldots, T\} \tag{8}$$

where $T \geq 1$ is a time horizon of the environment for the simulation, during which period an agent can take actions. For instance, if the time horizon $T = 24$ h and the time slot $t = 1$ h, the set has 24 elements in it.

These definitions are used in the following design of agent simulation.

A. Home Agent

The environment of an HA includes real-time prices P, real-time load L, real-time constraint set ct, dissatisfaction factor set λ^{ap}, and DLC signals DLC

$$\mathcal{E}_{\text{HA}} = \{P, L, \text{ct}, \lambda^{\text{ap}}, \text{DLC}\} \tag{9}$$

where P and L are defined as column vectors of the electricity price and the household load in each time slot in (10) and (11), respectively. ap represents an appliance in a home. λ^{ap} is a set of factors to reflect dissatisfaction levels of a customer to schedule the appliance ap. DLC represents load control signals from an RA. ct is a set of constraints; for instance, total electricity demands at any given time (slot) in a home cannot exceed a certain capacity $Q_{\text{HA}}^{\max}$. Other constraints are discussed in Section III-C in detail

$$P = <p_1, \ldots, p_T> \tag{10}$$

where the element p_t in the price vector P is the electricity price at time t

$$L = < \sum_{\text{ap} \in \mathcal{AP}} l_1^{\text{ap}}, \ldots, \sum_{\text{ap} \in \mathcal{AP}} l_T^{\text{ap}} > \tag{11}$$

where the household load L is the aggregation of all the appliances in a home. $\mathcal{AP}$ is a set of the appliances in a home. l_t^{ap} is the load of the appliance ap $\in \mathcal{AP}$ at time $t \in \mathcal{T}$. $\sum_{\text{ap} \in \mathcal{AP}} l_t^{\text{ap}}$ is the aggregated appliance loads at time t.

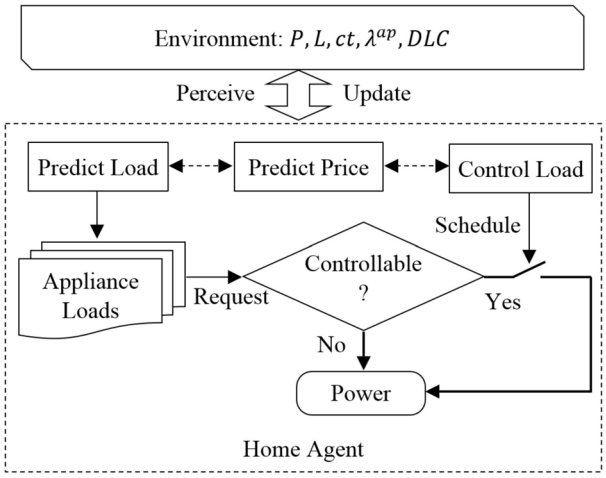

Fig. 2. HA is a model of a smart home, which includes load and price prediction and load control.

HAs have three types of actions

$$\mathcal{AC}_{\text{HA}} = \{\text{predict load}, \text{predict price}, \text{control load}\} \tag{12}$$

where predict load and predict price refer to forecasting real-time household loads and real-time electricity prices, respectively. The control load action schedules the load.

Fig. 2 shows the architecture of an HA, which predicts an individual appliance load. If the load is controllable (e.g., EV charging), the electricity demand is scheduled by the control load action. If the load of the appliance is not controllable (e.g., lighting), it is connected to the power line immediately. The objective of the control load action is to determine an optimal set of $\mathcal{AC}_{\text{HA}}^{\star}$ to minimize electricity payment based on predicted real-time prices and/or DLC request. The optimal $\mathcal{AC}_{\text{HA}}^{\star}$ is essentially a sequence of operational signals for all controllable loads under certain constraints.

The mechanism to predict electricity prices and the models to predict and control the load are discussed in Section III.

B. Retailer Agent

The characteristics of an RAs environment include real-time electricity prices P, service scope $\mathcal{RS}$, aggregated loads $\sum_{\text{HA} \in \mathcal{RS}} L_t^{\text{HA}}, \forall t \in \mathcal{T}$, available power Q_{RA}, and the max-power capacity $Q_{\text{RA}}^{\max}$

$$\mathcal{E}_{\text{RA}} = \left\{ P, \mathcal{RS}, \sum_{\text{HA} \in \mathcal{RS}} L_t^{\text{HA}}, Q_{\text{RA}}, Q_{\text{RA}}^{\max} \right\}. \tag{13}$$

The actions for an RA are as follows:

$$\mathcal{AC}_{\text{RA}} = \big\{\text{aggregate load}, \text{predict wholesale price}, \text{purchase}, \text{sell}, \text{DLC}\big\}. \tag{14}$$

Fig. 3 shows the RA architecture. An RA aggregates power demand of the HAs in its service area and purchases power from an electricity wholesale market. The RA then sells power to the HAs in a retail market. Under certain conditions such as transmission constraints, abundant renewable energy, and power shortage, the RA may request DLC, which is a set of time sequences $\mathcal{T}_{\text{DLC}}$.

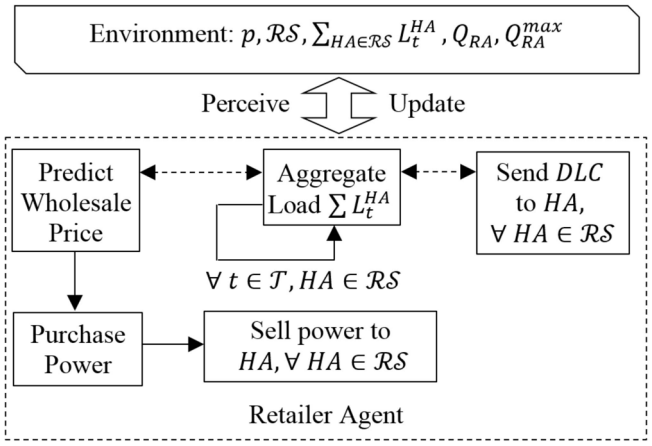

Fig. 3. RA is a model of an electricity retailer or a utility, which includes wholesale electricity price prediction, load aggregation, purchase and sell/delivery power, and DLC.

C. Wholesale Market Agent and Generator Agent

This paper focuses on optimal residential DR in a distribution network; therefore, WMA and GA are only briefly introduced. RAs request energy from the WMA, and GAs bid capacity in the WMA. The generation capacity with the lowest price will be assigned first in the market. Finally, the market reaches a steady state and a marginal price is achieved based on transmission constraints to different locations.

D. Common Features of Agents

In order to execute an MAS, an agent execution environment is required. For instance, java agent development framework provides an environment to develop agent systems compatible with the Foundation for Intelligent Physical Agents protocols [42]. The TRlabs Execution Environment for Mobile Agents (TEEMA) is adopted as the platform in this paper because of its familiarity to Wang and Paranjape [43], [44]. TEEMA provides standard libraries to support various types of operations for agents such as addressing, naming, messaging, mobility, security, and logging [45]. Either of these tools can be used to implement this system.

III. Mathematical Models

A. Real-Time Price Prediction Model

There are several dynamic tariffs that have been implemented in residential sectors. For instance, BH uses IBR [4]. The electricity prices vary between 7.52 ¢/kWh and 11.27 ¢/kWh based on energy consumption. If the amount of consumption in a 2-month billing period is below 1350 kWh, customers pay the first step price (7.52 ¢/kWh); otherwise, the price is 11.27 ¢/kWh in the second step (effective April 1, 2014). Fig. 4 shows the electricity payment with energy consumption. The solid blue lines show the payment linearly increases with amount of energy consumption. The slope of the first segment is the step 1 price 7.52 ¢/kWh. Once the energy exceeds the threshold, the slope becomes the step 2 price 11.27 ¢/kWh. For the purpose of optimization,

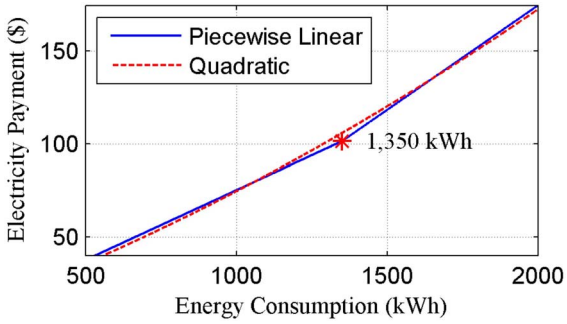

Fig. 4. Electricity payment with energy consumption [12].

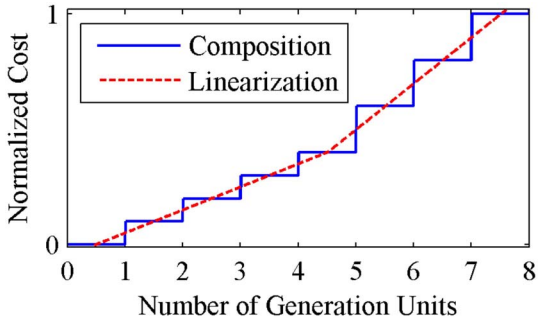

Fig. 5. Normalized composited generation cost with respect to the mix of the generation units.

these piecewise linear functions can be smoothed by a quadratic function shown by the red-dashed line [12].

The electricity demand is highly variable and also the electricity cannot be economically stored; therefore, a mix of power generation plants/units (e.g., hydro, nuclear, coal, oil, gas, and peaking hydro) is used to meet the demand [46]. Each type of plants also has a number of units. These plants/units are dispatched mainly based on their generation cost [46]. In addition, once the demand exceeds the base load, the generation cost of the units (e.g., gas and peaking hydro) to meet the peak demand increases faster. These characteristics of the composited generation cost with respect to the mix of the generation units to meet the demand can be captured by step functions (as shown by the blue lines in Fig. 5).

We define piecewise linear functions in the following equation as the price prediction model to linearize (see red-dashed line in Fig. 5) these steps:

$$p(l_t) = \begin{cases} \alpha_1 l_t + \beta_1, & \forall\, l_t \le l_{\mathrm{TH}}, t \in T \\ \alpha_2 l_t + \beta_2, & \forall\, l_t > l_{\mathrm{TH}}, t \in T \end{cases} \tag{15}$$

where α_1 is the slope of electricity price in the first step ($l_t \le l_{\mathrm{TH}}$) and α_2 is the slope in the second step where $l_t > l_{\mathrm{TH}}$. β_1 and β_2 are constants. Also, $\alpha_1 < \alpha_2$ implies the electricity price increases faster after the load exceeds the threshold l_{TH}. The coefficients are obtained by the norm approximation from historical data. The predicted RTP using the proposed model reveals the generation cost and encourages customers to redistribute the electricity usage, which would reduce peak demand and result in a more flat load profile.

Fig. 6 shows the actual electricity load and locational marginal price (LMP) in the wholesale market in the region of

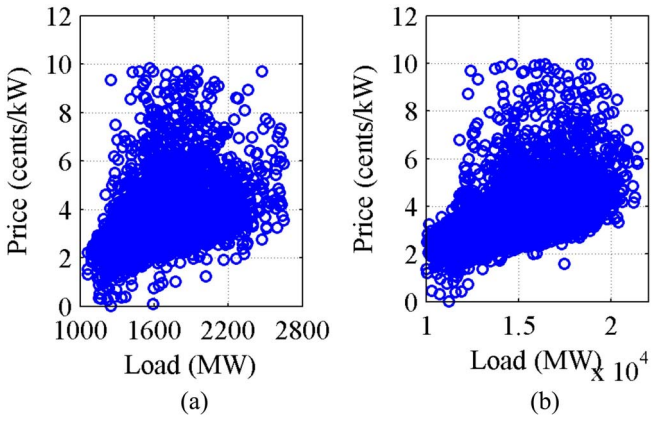

Fig. 6. Actual electricity load and LMP (wholesale) in regions of the U.S. in the year of 2014. (a) Region of DUQ. (b) Region of AEP [41].

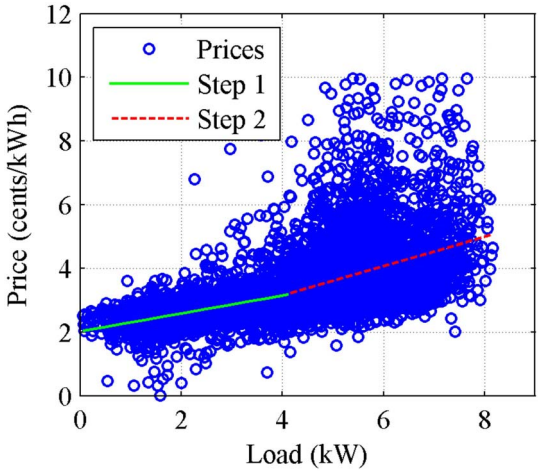

Fig. 7. Linear regression of load and electricity prices.

duquesne light (DUQ) and American Electric Power (AEP) of the U.S. in the year of 2014 [41]. We can see that the LMP has the same range and pattern increasing with the electricity load. However, the load in the region of DUQ (approximately from 1×10^3 MW to 2.8×10^3 MW) is much less than the region of AEP (approximately from 1×10^4 MW to 2.2×10^4 MW). Therefore, the electricity price does not directly depend on the absolute demand as long as the transmission constraint is satisfied. In this paper, we use the load and price data in the region of AEP as samples; however, the load is normalized and scaled in order to fit our simulation. For instance, to predict the electricity price-based individual household load, the load range is normalized and scaled from 0 to 8.5 kW, which is the range of power load in a typical home with an EV in place.

The norm approximation is used to determine the parameters in (15) using these normalized data and then predict electricity price by given load demand. This can be solved by using Newton's method [47, pp. 525–531]. Fig. 7 shows an example of prediction results. The blue circles are the real-time LMP corresponding to the real-time load demand. The blue solid line shows the prediction in the first step and the red-dashed line shows the second step.

In this paper, we do not intend to explore this linear regression technique. One can divide the data into several groups; use one of them to train the parameters and evaluate the degree of error using other groups.

B. Residential Load Prediction Model

We develop a residential load prediction model, which incorporates 19 appliances/loads including vacuum, hob, oven, microwave, kettle, TV, iron, refrigerator, CD player, clock, answering machine, Wi-Fi, PC, printer, light, clothes washer/dryer, dish washer, and EV.

An individual appliance load is defined as follows:

$$l_t^{\text{ap}} = q_{\text{rated}}^{\text{ap}}, \quad \forall \text{ap} \in \mathcal{AP}, t \in \left[t_0^{\text{ap}}, t_0^{\text{ap}} + \Delta t^{\text{ap}}\right] \tag{16}$$

$$l_t^{\text{ap}} = 0, \quad \forall \text{ap} \in \mathcal{AP}, t \in \mathcal{T} \backslash \left[t_0^{\text{ap}}, t_0^{\text{ap}} + \Delta t^{\text{ap}}\right] \tag{17}$$

where l_t^{ap} is the load of an appliance ap at a time slot t. $q_{\text{rated}}^{\text{ap}}$ is the rated power of the appliance. t_0^{ap} is the time of starting to operate an appliance ap [as shown in (18)]. Δt^{ap} is a cycle length of operating the appliance. An appliance may operate multiple cycles (e.g., refrigerator) in the horizon T. The power of an appliance is zero when it is not used and we also assume that the appliance standby power is zero [as shown in (17)]

$$t_0^{\text{ap}} \leftarrow \text{pr}(t|\text{ap}, [\text{occ}(t)]), \forall \text{ap} \in \mathcal{AP} \backslash \text{EV} \tag{18}$$

where $\text{pr}(t|\text{ap}, [\text{occ}(t)])$ is the probability of using an appliance ap $\in \mathcal{AP}\backslash\text{EV}$ at a time slot t. $\text{occ}(t)$ represents the number of active occupants at t in a home, which has an influence on the probability of operating appliances. Usually, an occupant is required to start an appliance; however, some appliances (e.g., refrigerator) operate on their own cycle. This option is shown by the square bracket around $\text{occ}(t)$. The operation of the refrigerator does not depend on the using probability. However, a corresponding "probability" is calculated as the reciprocal of the mean time excluding the running/delaying time between the consecutive starting events. Except parameters for the EV, the values of $\text{pr}(t|\text{ap}, [\text{occ}(t)])$, $\text{occ}(t)$, Δt^{ap}, and $q_{\text{rated}}^{\text{ap}}$ are derived from statistical information in the downloadable model of [48] and [49].

The mechanism for predicting an appliance's initial operating time t_0^{ap} is that the model generates a random number that follows a uniform distribution between 0 and 1 and compares this random number with the scaled probability of running an appliance at time t [as shown by the right side of (18)]. If the random number is less than or equal to the probability, the appliance will be running in a cycle of Δt_{ap}; otherwise, it will not. Electricity consumption of all appliances is then aggregated. This process is repeated in the horizon T.

We now discuss the parameters for EV charging. Assuming people plug-in and charge EVs immediately after arriving home, the probability distribution of initial charging time is the same as home-arrival time. This probability of initial charging time is formulated as a normal distribution $t_0^{\text{ap}} \sim \mathcal{N}(\mu_{t0}, \sigma_{t0}), \forall \text{ap} = EV$, which is discussed in detail in [50] and [51]. EVs must be fully charged in order to be used the next day. The home-departure time is assumed to be normally distributed as discussed in Section IV.

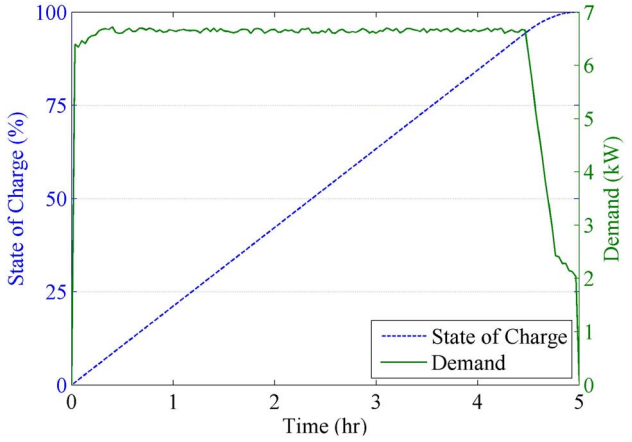

Fig. 8. SOC and demand of Nissan Altra-EV with lithium-ion battery [53].

The cycle length $\Delta t^{\text{ap}}, \forall \text{ap} = \text{EV}$ depends on the battery's SOC, which is defined as the remaining capacity over the rated capacity [52]. Fig. 8 shows SOC and demand with charging time of a Nissan Altra-EV with a lithium-ion battery [53].

The initial SOC soc_0 when an EV is plugged-in can be identified as a normal distribution $\text{soc}_0 \sim \mathcal{N}(\mu_{\text{soc}}, \sigma_{\text{soc}})$ from driving patterns [50]. Since available EV travel range is proportional to its SOC [53], the average soc_0 can be calculated by: $\mu_{\text{soc}} = (\text{Range} - \text{DVM})/\text{Range}$, where Range is the available driving range of a fully charged vehicle. DVM is average daily vehicle miles, which means the average driving miles per vehicle per day. Similarly, σ_{soc} can be calculated from the standard deviation of DVM. A detailed discussion can be found in [50].

The cycle length $\Delta t^{\text{ap}}, \forall \text{ap} = \text{EV}$ can be calculated as follows:

$$\Delta t^{\text{ap}} = \Delta t_{\text{total}}(1 - \text{soc}_0), \forall \text{ap} = \text{EV} \tag{19}$$

where Δt_{total} is the time to charge up an EV from zero SOC.

Lastly, we divide the set of appliances $\mathcal{AC}$ into two sets: 1) $\mathcal{BAP}$; and 2) $\mathcal{CAP}$, which represent a set of background appliances and controllable appliances, respectively.

The predicted load is shown in the following equation:

$$\hat{L} = <\widehat{l_1^{\text{ap}}}, \ldots, \widehat{l_T^{\text{ap}}}>. \tag{20}$$

Predicted energy is defined as follows:

$$\widehat{E_B^{\text{ap}}} = \sum_t \widehat{l_t^{\text{ap}}}, \forall \text{ap} \in \mathcal{BAP}, t \in [t_0^{\text{ap}}, t_0^{\text{ap}} + \Delta t^{\text{ap}}] \tag{21}$$

$$\widehat{E_C^{\text{ap}}} = \sum_t \widehat{l_t^{\text{ap}}}, \forall \text{ap} \in \mathcal{CAP}, t \in [t_0^{\text{ap}}, t_0^{\text{ap}} + \Delta t^{\text{ap}}] \tag{22}$$

where $\widehat{E_B^{\text{ap}}}$ and $\widehat{E_C^{\text{ap}}}$ are the predicted electricity energy of background loads and controllable loads. It is noted that both $\widehat{E_B^{\text{ap}}}$ and $\widehat{E_C^{\text{ap}}}$ are the column vectors (e.g., $\widehat{E_B^{\text{ap}}} = <\widehat{E_{B,1}^{\text{ap}}}, \ldots, \widehat{E_{B,T}^{\text{ap}}}>$).

C. Load Control Model

Load control action provides the ability for an HA to make intelligent decisions to minimize electricity payments, which is modeled by a CP problem

minimize

$$\sum_{t \in \mathcal{T}} p\left(\sum_{\text{ap} \in \mathcal{AP}} l_t^{\text{ap}}\right)\left(\sum_{\text{ap} \in \mathcal{AP}} l_t^{\text{ap}}\right) + \sum_{t \in \mathcal{T}} \sum_{\text{ap} \in \mathcal{CAP}} \lambda^{\text{ap}} w^{\text{ap}} l_t^{\text{ap}}$$

subject to

$$0 \le l_t^{\text{ap}} \le q_{\text{rated}}^{\text{ap}}, \forall \text{ap} \in \mathcal{CAP}, t \in [t_0^{\text{ap}}, t_1^{\text{ap}}] \tag{c1}$$

$$l_t^{\text{ap}} = 0, \forall \text{ap} \in \mathcal{CAP}, t \in \mathcal{T} \backslash [t_0^{\text{ap}}, t_1^{\text{ap}}] \tag{c2}$$

$$\sum_{\text{ap}} \sum_t l_t^{\text{ap}} = \widehat{E_C^{\text{ap}}}, \forall \text{ap} \in \mathcal{CAP}, t \in [t_0^{\text{ap}}, t_1^{\text{ap}}] \tag{c3}$$

$$\sum_{\text{ap} \in \mathcal{CAP}} l_t^{\text{ap}} + \sum_{\text{ap} \in \mathcal{BAP}} \widehat{l_t^{\text{ap}}} \le Q_{\text{HA}}^{\max}, \forall t \in \mathcal{T}. \tag{c4}$$

In the objective function, the electricity price $p(\sum_{\text{ap} \in \mathcal{AP}} l_t^{\text{ap}})$ is defined in (15), which is a piecewise linear function with load. The electricity payment $\sum_{t \in \mathcal{T}} p(\sum_{\text{ap} \in \mathcal{AP}} l_t^{\text{ap}})(\sum_{\text{ap} \in \mathcal{AP}} l_t^{\text{ap}})$ is a piecewise linear function times its independent variable load, which is a piecewise quadratic function. Each quadratic function is convex; furthermore, we have $\alpha_1 < \alpha_2$ and the convexity is preserved. The second term is a linear function of load l_t^{ap}, where λ^{ap} is a vector of dissatisfaction factors and w^{ap} is a waiting time vector defined as follows:

$$w^{\text{ap}} = t - t_0^{\text{ap}}. \tag{23}$$

For instance, if the EV plug-in time $t_0^{\text{ap}} = 17$ h, $\forall \text{ap} = \text{EV}$, the waiting time vector along with time is shown as follows:

w^{ap}	0	1	2	3	...
t	17hr	18hr	19hr	20hr	…

Since we minimize $\sum_{t \in \mathcal{T}} \sum_{\text{ap} \in \mathcal{CAP}} \lambda^{\text{ap}} w^{\text{ap}} l_t^{\text{ap}}$, an earlier operating time is more preferable. This term penalizes the scheduling levels to find the tradeoff between the minimum electricity payment and comfort levels with waiting time.

The decision variables are $l_t^{\text{ap}}, \forall \text{ap} \in \mathcal{CAP}, t \in \mathcal{T}$. In the objective function, $l_t^{\text{ap}}, \forall \text{ap} \in \mathcal{BAP}$ are not decision variables; however, they are required to calculate the electricity payment.

The first constraint is a relaxation of a binary constraint, in which $l_t^{\text{ap}} \in \{0, q_{\text{rated}}^{\text{ap}}\}$, which results in that the optimization problem can be solve much more efficiently. t_0^{ap} is the appliance usage requesting time and t_1^{ap} is the time when operation of the appliance must complete. $[t_0^{\text{ap}}, t_1^{\text{ap}}]$ is a possible operational range of the controllable appliance ap. For instance, an EV can be charged from the home-arrival time to home-departure time. We assume that the controllable load can only be delayed.

The second constraint (c2) sets the load of an appliance to be zero when it is not operating. Although, operating a controllable appliance could be delayed, it completes sooner or later in the operational range; therefore, it consumes the same energy as predicted. This fact is accomplished in the third constraint (c3). The (c4) constraint is that the max-power capacity of a home cannot be violated at any given time.

The objective function is a piecewise quadratic function with preserved convexity plus a linear function; therefore, the

TABLE I
COEFFICIENTS OF THE PRICE PREDICTION MODEL

Parameter	α_1	β_1	α_2	β_2
Single Home	0.282	2.025	0.459	1.317
100 Homes	0.015	1.776	0.025	0.911

objective function is convex. In addition, all the constraints are affine functions. Therefore, the proposed optimization problem is a CP problem, which can be solved efficiently by the interior point method [47]. To solve this CP problem, we used CVX, a package for specifying and solving convex programs [54], [55].

If the HA receives DLC signals, the CP problem has one more constraint (c5) assuming the DLC is to request a load reduction

$$l_t^{\text{ap}} = 0, \forall \text{ap} \in \mathcal{CAP}, t \in \mathcal{T}_{\text{DLC}}. \quad \text{(c5)}$$

With the constraint (c5), the new CP problem is not guaranteed to be feasible, since if the schedule does not have sufficient flexibilities, an HA may not able to accept the DLC request. If the CP problem is infeasible, the HA needs to determine the maximum power that can be shifted from the $\mathcal{T}_{\text{DLC}}$.

IV. SIMULATION RESULTS

This section presents simulation results for four scenarios.

1) *Without Load Control:* The HAs do not take actions to control load. This is the reference scenario in this paper.
2) *With Day-Ahead RTP:* The RA announces real-time prices one day ahead and will charge the HAs with the announced prices.
3) *With RTP Prediction:* The HAs are able to predict electricity prices. The HAs are charged by actual wholesale electricity prices based the aggregated load. This scenario assumes the dissatisfaction factor is zero.
4) *With RTP Prediction:* This scenario is designed to study the effect of dissatisfaction factor on load schedule.

A. Experimental Configurations

In all the scenarios, we consider one RA and 100 HAs in a distribution network. We assume that the RA can obtain sufficient power from a wholesale market and all transmission constraints are satisfied. We also assume that the retail market is budget balanced, i.e., the RA does not make profits. The power capacity of each HA is $Q_{\text{HA}}^{\max} = 24$ kW. The simulation period is one day. The time slot $t = 1$ h and time horizon $H = 24$ h. The coefficients for the price prediction model are listed in Table I.

Twenty HAs are equipped with an EV, which represents a 20% EV penetration to the power system. Among the appliances, dish washers, tumble dryers, and EVs are identified as controllable load. In the first three scenarios, we assume $\lambda^{\text{ap}} = 0$. In scenario #4, the dissatisfaction factor is studied using EV load as an example. Detail parameters of the controllable load are summarized in Table II. Parameters of the background load can be found in the downloadable excel sheet [48].

TABLE II
PARAMETER CHARACTERISTICS OF THE CONTROLLABLE LOADS

	q_{rated}^{ap}	t_0^{ap}	t_1^{ap}
Dish washer	1.1 kW	Determined by Equation (18)	t_0^{ap} + 4 hours for breakfast/lunch; 6hr for dinner
Dryer	2.5 kW	Determined by Equation (18)	t_0^{ap} + 24 hours
EV	6.6 kW	Normal distribution with $\mu = 17hr$ and $\sigma = 2.8\ hour$	Normal distribution with $\mu = 7hr$ and $\sigma = 1\ hour$

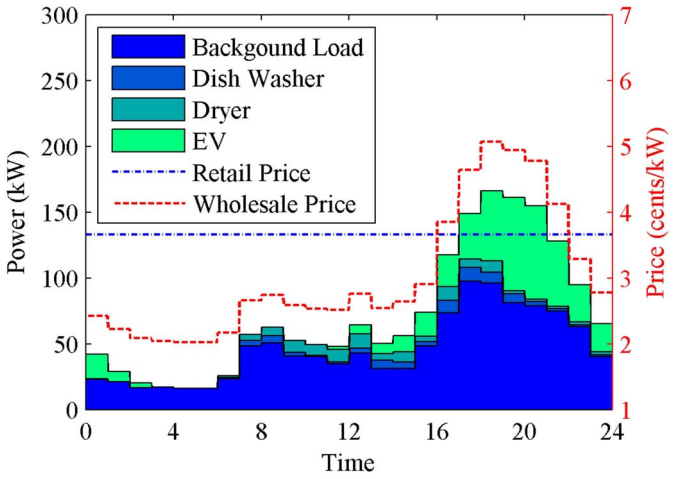

Fig. 9. Load profile of aggregation of 100 HAs, retail electricity prices, and wholesale electricity prices in scenario #1.

The results of electricity payments of HAs are grouped in terms of ownership of EVs, which make the results comparable, since EV charging represents a significant demand.

B. Scenario #1

This scenario is the reference in this paper. The HAs do not take any actions to control load. Fig. 9 shows the simulation results in this scenario. The wholesale electricity price is shown by the red-dashed line. The blue dash-dotted line shows the equivalent flat electricity rate in the retail market assuming a budget-balanced market.

We now discuss the method of calculating the equivalent flat rate. The energy consumption was 1716.9 kWh. To purchase this amount of energy from the wholesale market, the retailer spent \$62.77 based on the wholesale price. The HAs are charged by the flat rate. To keep the budget balanced, the equivalent flat rate is calculated as follows \$62.77/1716.9 kWh = 3.66 ¢/kWh.

The individual HAs electricity bills are shown by the blue circles in Fig. 12. The average electricity payments of the

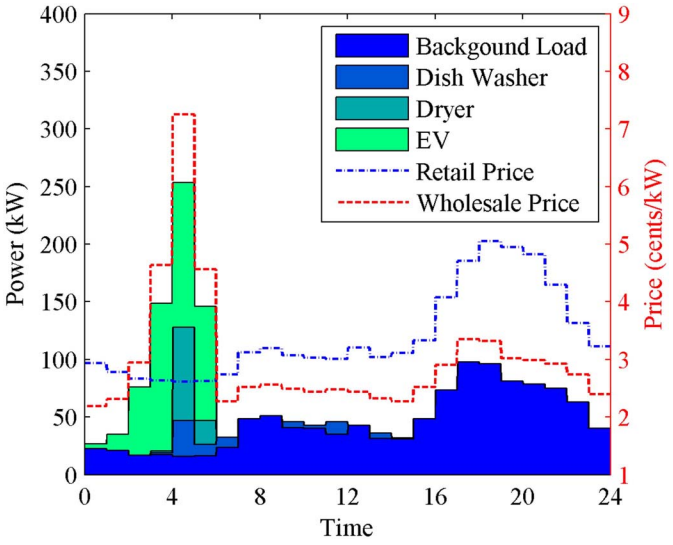

Fig. 10. Load profile of aggregation of 100 HAs, retail electricity prices, and wholesale electricity prices in scenario #2.

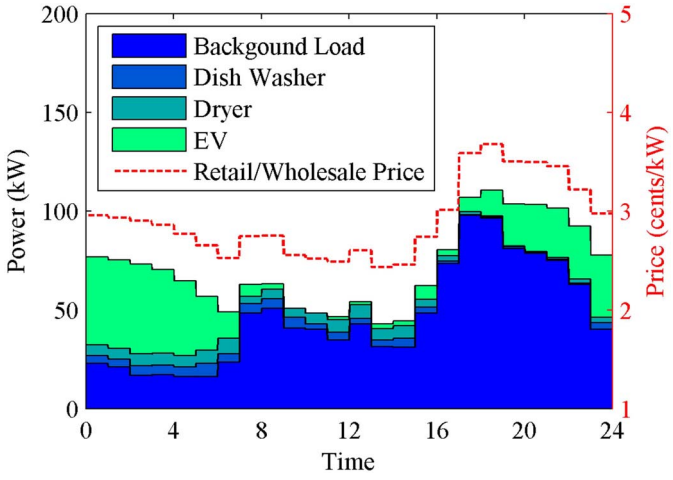

Fig. 11. Load profile of aggregation of 100 HAs, retail electricity prices, and wholesale electricity prices in scenario #3.

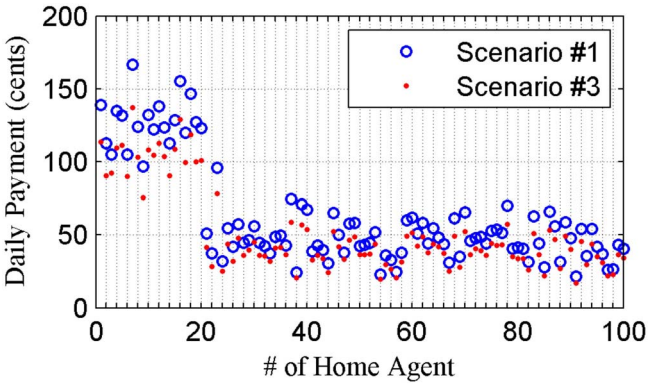

Fig. 12. Electricity payment (100 Has) in scenarios #1 and #3.

HAs that own an EV was \$1.27. The maximum and minimum electricity bill was \$1.66 and \$0.97, respectively. The electricity payment of the HAs without an EV was \$0.47 (average), \$0.96 (maximum), and \$0.21 (minimum).

The PAPR was 2.32 and the standard deviation of the load profile was 47.7 kW. The usages of controllable loads are as follows: 25 usages of dish washer, 33 usages of dryers, and 20 usages of EVs. In addition, there were 24 HAs who did not use controllable load in the simulation day. The same predicted energy consumption was used for the other scenarios to make them comparable and reproducible.

C. Scenario #2

This scenario considers a situation where the real-time price is announced one day ahead and the HAs can manage electricity consumption accordingly. This means that the RA will charge the HAs based on the announced price regardless of the actual wholesale price in the next day.

The HAs scheduled the controllable load based upon the day-ahead announced real-time price by solving the optimization problem as shown in Section III-C. The CP problem becomes an LP problem since the electricity price was provided with respect to time rather than a function of load.

Fig. 10 shows the simulation results. The blue dash-dotted line shows the day-ahead announced electricity price that acts as the retail electricity price to charge the HAs. The aggregated load generated a higher new peak demand in the lowest price period. The red-dashed line shows the actual wholesale electricity price based on the scheduled load profile. The PAPR and the standard deviation were increased to 3.54 and 50.7 kW, respectively.

In addition, the total electricity payment from the HAs was \$51.56. However, to purchase the electricity energy from the wholesale market using the actual wholesale price, the retailer needs \$64.25. Apparently, this market cannot be budget-balanced.

D. Scenario #3

In this scenario, the HAs have ability to predict electricity prices using the price prediction model. The RA charged the HAs by the actual wholesale electricity price, i.e., the wholesale price was the same as the retail price. The simulation was conducted using a MacBook Pro with a 2.4 GHz Intel Core i5 processor and 8 GB of RAM memory. The computational time for solving the CP problem is about 0.4 s for a single HA.

The HAs scheduled the controllable load to minimize the electricity payment. Fig. 11 shows the simulation results. Both the RA and the HAs benefited from a reduced electricity payment of \$51.82. The PAPR was reduced to 1.54. The standard deviation was also decreased to 21.6 kW.

Fig. 12 shows daily electricity bills comparing with scenario #1. The average electricity payment of the HAs that own an EV was \$1.05, which was reduced by 17.5%. They had the maximum payment of \$1.37 with a reduction of 21.9% and the minimum payment of \$0.76 with a reduction of 12.3%. The HAs without an EV also benefited from the decreased bills of \$0.39 (average), \$0.78 (maximum), and \$0.17 (minimum). The average, maximum, and minimum percentage of decrease was 17.4%, 24.3%, and 12.3%, respectively.

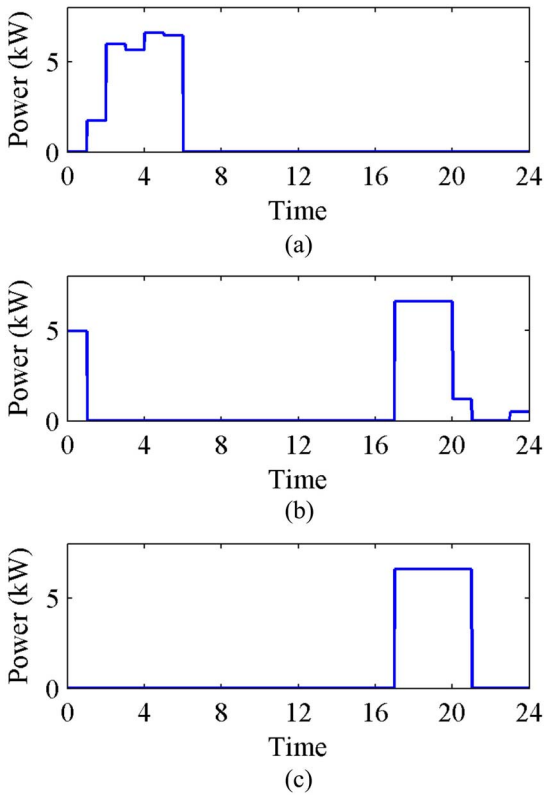

Fig. 13. Scheduled EV load with different dissatisfaction factors. (a) $\lambda^{ap} = 0$. (b) $\lambda^{ap} = 0.4$. (c) $\lambda^{ap} = 0.8$.

E. Scenario #4

This scenario evaluates the impact of dissatisfaction factor on the load schedule. We use an EV of an HA as an example of controllable load and consider other loads as background loads to emphasize the effectiveness of the dissatisfaction factor. The plug-in time and must completed time of the EV were assumed at 17 P.M. and 7 A.M., respectively. The initial SOC was 20%, which means the EV requires 4 h to be fully charged. The background load profile is shown in the previous scenarios.

Fig. 13 shows scheduled EV load using different dissatisfaction factors of 0, 0.4, and 0.8. From Fig. 13(a), we can see that the load is scheduled to the off-peak demand period to minimize the electricity payment without consideration of waiting time since the dissatisfaction factor is 0. By contrast, with dissatisfaction factor of 0.8, the EV load could not be scheduled as shown in Fig. 13(c) since this high dissatisfaction factor represents the user preference to charge the EV immediately. Fig. 13(b) shows the situation where the dissatisfaction was 0.4, in which the solution is a tradeoff between electricity payment and waiting time.

Fig. 14 shows the electricity payment versus waiting time using different dissatisfaction factors for a single EV. With increasing lambda from 0 to 0.8, the daily electricity payment for a single EV increases from 74 to 94 cents while the waiting time decreases from 10 to 0 h. The waiting time is calculated as follows:

$$\text{waiting time} = \text{completion time} - \text{plugin time} - \text{required charging time}.$$

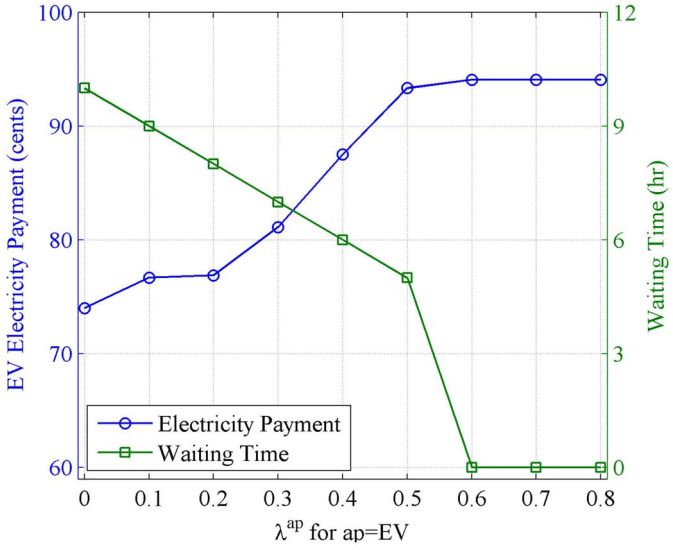

Fig. 14. Electricity payment versus waiting time using different dissatisfaction factors for a single EV.

TABLE III
COMPARISON OF THE OBSERVATIONS IN SCENARIOS #1 AND #3

Scenario	Obs	PAPR	Standard Deviation (kW)	Total Payment ($)
#1		2.32	47.7	62.77
#3		1.54	21.6	51.82

TABLE IV
SUMMARY OF THE INDIVIDUAL ELECTRICITY PAYMENT IN SCENARIOS #1 AND #3

	Have EVS	Electricity Payment ($)			Payment Reduction (%)		
		Average	Max	Min	Average	Max	Min
#1	Yes	1.27	1.66	0.97	-	-	-
	No	0.47	0.96	0.21	-	-	-
#3	Yes	1.05	1.37	0.76	17.5	21.9	12.3
	No	0.39	0.78	0.17	17.4	24.3	12.3

For instance, if the plugin time is 17 h, the fully charged time is 21 h; and required charging-up time is 4 h (i.e., it requires 4 h to fully charge the EV), and the waiting time is zero.

V. DISCUSSION

This section compares and discusses the four scenarios. We discuss scenario #2 first. The total electricity payment from the HAs is $51.56. However, the RA spends $64.25 on purchasing the electricity energy. Apparently, the market cannot be budget-balanced. In general, although a customer's individual electricity payment can be reduced using day-ahead RTP, it is not a feasible plan if the customers are able to schedule the load accordingly.

Table III summarizes the observations of the PAPR, the standard deviation, and the total electricity payment in scenarios #1 and #3. We can see that in scenario #3, the PAPR, standard deviation, and electricity payment decrease.

Table IV illustrates the individual electricity payment from the HAs in scenarios #1 and #3. In both the scenarios,

the electricity payment of the HAs with an EV is higher than the HAs without an EV since EV charging represents a significant electricity demand. However, we can see that all HAs benefit from a reduced electricity payment with DR using the proposed mechanism regardless of controllable load usage, amount of energy consumed, or EV ownership. It is noted that, in the experiments, there were 24 HAs who did not use controllable loads in the simulation day and 80% of homes do not own an EV. This demonstrates the fairness of using the proposed mechanisms for all users.

In scenario #3, the HAs solve an optimization problem to minimize the electricity payment based on the predicted electricity price. The scheduled electricity load is significantly better than without load control. In addition, the HAs do not expose the electricity usage to the other HAs. Furthermore, it does not require coordination among HAs.

Scenario #4 shows effects of dissatisfaction factor λ^{ap} on scheduling the EV load. We can see that the electricity payment increases while the waiting time decreases with increasing the dissatisfaction factor. Users can determine a "best" value for the dissatisfaction factor to find a tradeoff between electricity payment and waiting time.

The optimal control of electricity consumption is evaluated in a simulation environment in this paper. It can also be extended into a real-time environment, where the load prediction of the HA is replaced by real-time actual electricity consumption and the CP problem is solved hourly. The wholesale electricity prediction of the RA can be also replaced by actual prices by incorporation of bidding from multiple generators.

VI. Conclusion

RTP as a DR policy has great potential to reduce electricity payments and improve the stability of the power system with DR implementation. However, responding to RTP requires DR enabling technologies. This paper proposes an optimal solution for responding to RTP in an agent-based simulation model for multiple heterogeneous homes. The HA is able to predict real-time load and real-time electricity prices. It can also intelligently control the electricity consumption to minimize electricity payment with consideration of waiting time by solving a CP problem. The RA can predict real-time wholesale electricity prices and operates DLC. Simulation results show that the PAPR and electricity payments are significantly reduced using the proposed algorithm under RTP. The propose simulation model can be a test-bed to evaluate various DR enabling technologies and policies. The HA, with the optimal control algorithm, can also be implemented in a home EMS to minimize the electricity payment.

References

[1] H. Chao, "Price-responsive demand management for a smart grid world," *Elect. J.*, vol. 23, no. 1, pp. 7–20, Feb. 2010.

[2] A. Conchado and P. Linares, "The economic impact of demand-response programs on power systems. A survey of the state of the art," in *Handbook of Networks in Power Systems I* (Energy Systems). Berlin, Germany: Springer-Verlag, 2012, pp. 281–301.

[3] Q. QDR, "Benefits of demand response in electricity markets and recommendations for achieving them," U.S. Dept. Energy, Washington, DC, USA, Tech. Rep. Feb. 2006.

[4] B. C. Hydro. (Feb. 3, 2015). *Residential Rates*. [Online]. Available: https://www.bchydro.com/accounts-billing/customer-service-residential/residential-rates.html

[5] Z. Wang, R. Paranjape, A. Sadanand, and Z. Chen, "Residential demand response: An overview of recent simulation and modeling applications," in *Proc. IEEE Can. Elect. Comput. Eng. Conf.*, Regina, SK, Canada, May 2013, pp. 1–6.

[6] P. Vrba *et al.*, "A review of agent and service-oriented concepts applied to intelligent energy systems," *IEEE Trans. Ind. Informat.*, vol. 10, no. 3, pp. 1890–1903, Aug. 2014.

[7] L. G. Swan and V. I. Ugursal, "Modeling of end-use energy consumption in the residential sector: A review of modeling techniques," *Renew. Sustain. Energy Rev.*, vol. 13, no. 8, pp. 1819–1835, Oct. 2009.

[8] A. Grandjean, J. Adnot, and G. Binet, "A review and an analysis of the residential electric load curve models," *Renew. Sustain. Energy Rev.*, vol. 16, no. 9, pp. 6539–6565, Dec. 2012.

[9] S. Shao, M. Pipattanasomporn, and S. Rahman, "Development of physical-based demand response-enabled residential load models," *IEEE Trans. Power Syst.*, vol. 28, no. 2, pp. 607–614, May 2013.

[10] W. Zhang, J. Lian, C. Y. Chang, and K. Kalsi, "Aggregated modeling and control of air conditioning loads for demand response," *IEEE Trans. Power Syst.*, vol. 28, no. 4, pp. 4655–4664, Nov. 2013.

[11] J. Kondoh, L. Ning, and D. J. Hammerstrom, "An evaluation of the water heater load potential for providing regulation service," *IEEE Trans. Power Syst.*, vol. 26, no. 3, pp. 1309–1316, Aug. 2011.

[12] A.-H. Mohsenian-Rad and A. Leon-Garcia, "Optimal residential load control with price prediction in real-time electricity pricing environments," *IEEE Trans. Smart Grid*, vol. 1, no. 2, pp. 120–133, Sep. 2010.

[13] K. M. Tsui and S.-C. Chan, "Demand response optimization for smart home scheduling under real-time pricing," *IEEE Trans. Smart Grid*, vol. 3, no. 4, pp. 1812–1821, Dec. 2012.

[14] L. P. Qian, Y. J. A. Zhang, J. Huang, and Y. Wu, "Demand response management via real-time electricity price control in smart grids," *IEEE J. Sel. Areas Commun.*, vol. 31, no. 7, pp. 1268–1280, Jul. 2013.

[15] N. Gudi, L. Wang, and V. Devabhaktuni, "A demand side management based simulation platform incorporating heuristic optimization for management of household appliances," *Int. J. Elect. Power Energy Syst.*, vol. 43, no. 1, pp. 185–193, Dec. 2012.

[16] Y. Guo, M. Pan, and Y. Fang, "Optimal power management of residential customers in the smart grid," *IEEE Trans. Parallel Distrib. Syst.*, vol. 23, no. 9, pp. 1593–1606, Sep. 2012.

[17] T. Logenthiran, D. Srinivasan, and T. Z. Shun, "Demand side management in smart grid using heuristic optimization," *IEEE Trans. Smart Grid*, vol. 3, no. 3, pp. 1244–1252, Sep. 2012.

[18] P. Samadi, H. Mohsenian-Rad, R. Schober, and V. W. Wong, "Advanced demand side management for the future smart grid using mechanism design," *IEEE Trans. Smart Grid*, vol. 3, no. 3, pp. 1170–1180, Sep. 2012.

[19] M. A. A. Pedrasa, T. D. Spooner, and I. F. MacGill, "Coordinated scheduling of residential distributed energy resources to optimize smart home energy services," *IEEE Trans. Smart Grid*, vol. 1, no. 2, pp. 134–143, Sep. 2010.

[20] N. Li, L. Chen, and S. H. Low, "Optimal demand response based on utility maximization in power networks," in *Proc. IEEE Power Energy Soc. Gen. Meeting*, San Diego, CA, USA, Jul. 2011, pp. 1–8.

[21] T.-H. Chang, M. Alizadeh, and A. Scaglione, "Real-time power balancing via decentralized coordinated home energy scheduling," *IEEE Trans. Smart Grid*, vol. 4, no. 3, pp. 1490–1504, Sep. 2013.

[22] A. Safdarian, M. Fotuhi-Firuzabad, and M. Lehtonen, "A distributed algorithm for managing residential demand response in smart grids," *IEEE Trans. Ind. Informat.*, vol. 10, no. 4, pp. 2385–2393, Nov. 2014.

[23] Z. Baharlouei, M. Hashemi, H. Narimani, and H. Mohsenian-Rad, "Achieving optimality and fairness in autonomous demand response: Benchmarks and billing mechanisms," *IEEE Trans. Smart Grid*, vol. 4, no. 2, pp. 968–975, Jun. 2013.

[24] J. Vardakas, N. Zorba, and C. Verikoukis, "A survey on demand response programs in smart grids: Pricing methods and optimization algorithms," *IEEE Commun. Surveys Tuts.*, vol. 17, no. 1, pp. 152–178, Jul. 2014.

[25] M. Wooldridge, *An Introduction to Multiagent Systems.* Hoboken, NJ, USA: Wiley, 2009.

[26] S. D. McArthur *et al.*, "Multi-agent systems for power engineering applications—Part I: Concepts, approaches, and technical challenges," *IEEE Trans. Power Syst.*, vol. 22, no. 4, pp. 1743–1752, Nov. 2007.

[27] H. S. V. S. Kumar Nunna and S. Doolla, "Energy management in microgrids using demand response and distributed storage—A multi-agent approach," *IEEE Trans. Power Del.*, vol. 28, no. 2, pp. 939–947, Apr. 2013.
[28] J. Bingnan and F. Yunsi, "Smart home in smart microgrid: A cost-effective energy ecosystem with intelligent hierarchical agents," *IEEE Trans. Smart Grid*, vol. 6, no. 1, pp. 3–13, Jan. 2015.
[29] S. Kahrobaee, R. A. Rajabzadeh, L.-K. Soh, and S. Asgarpoor, "A multi-agent modeling and investigation of smart homes with power generation, storage, and trading features," *IEEE Trans. Smart Grid*, vol. 4, no. 2, pp. 659–668, Jun. 2013.
[30] Z. Wang and R. Paranjape, "Agent-based simulation of home energy management system in residential demand response," in *Proc. IEEE Canadian Elect. Comput. Eng. Conf.*, Toronto, ON, Canada, May 2014, pp. 1–6.
[31] P. Papadopoulos, N. Jenkins, L. M. Cipcigan, I. Grau, and E. Zabala, "Coordination of the charging of electric vehicles using a multi-agent system," *IEEE Trans. Smart Grid*, vol. 4, no. 4, pp. 1802–1809, Dec. 2013.
[32] E. L. Karfopoulos and N. D. Hatziargyriou, "A multi-agent system for controlled charging of a large population of electric vehicles," *IEEE Trans. Power Syst.*, vol. 28, no. 2, pp. 1196–1204, May 2013.
[33] C.-X. Dou and B. Liu, "Multi-agent based hierarchical hybrid control for smart microgrid," *IEEE Trans. Smart Grid*, vol. 4, no. 2, pp. 771–778, Jun. 2013.
[34] Y. S. Foo Eddy, H. B. Gooi, and S. X. Chen, "Multi-agent system for distributed management of microgrids," *IEEE Trans. Power Syst.*, vol. 30, no. 1, pp. 24–34, Jan. 2015.
[35] H. S. V. S. K. Nunna and S. Doolla, "Demand response in smart distribution system with multiple microgrids," *IEEE Trans. Smart Grid*, vol. 3, no. 4, pp. 1641–1649, Dec. 2012.
[36] Y. Shoham and K. Leyton-Brown, *Multiagent Systems: Algorithmic, Game-theoretic, and Logical Foundations.* Cambridge, U.K.: Cambridge Univ. Press, 2008.
[37] W. Wei, L. Feng, and M. Shengwei, "Energy pricing and dispatch for smart grid retailers under demand response and market price uncertainty," *IEEE Trans. Smart Grid*, vol. 6, no. 3, pp. 1364–1374, May 2015.
[38] O. Kilkki, A. Alahaivala, and I. Seilonen, "Optimized control of price-based demand response with electric storage space heating," *IEEE Trans. Ind. Informat.*, vol. 11, no. 1, pp. 281–288, Feb. 2015.
[39] A.-H. Mohsenian-Rad, V. W. S. Wong, J. Jatskevich, R. Schober, and A. Leon-Garcia, "Autonomous demand-side management based on game-theoretic energy consumption scheduling for the future smart grid," *IEEE Trans. Smart Grid*, vol. 1, no. 3, pp. 320–331, Dec. 2010.
[40] P. Yang, G. Tang, and A. Nehorai, "A game-theoretic approach for optimal time-of-use electricity pricing," *IEEE Trans. Power Syst.*, vol. 28, no. 2, pp. 884–892, May 2013.
[41] PJM. (Feb. 3, 2015). *Real-Time Energy Market*. [Online]. Available: http://www.pjm.com/markets-and-operations/energy/real-time.aspx
[42] F. Bellifemine, F. Bergenti, G. Caire, and A. Poggi, "JADE—A java agent development framework," in *Multi-Agent Programming* (Multiagent Systems, Artificial Societies, and Simulated Organizations), vol. 15. New York, NY, USA: Springer, 2005, pp. 125–147.
[43] Z. Wang and R. Paranjape, "The self-aware diabetic patient software agent model," *Comput. Biol. Med.*, vol. 43, no. 11, pp. 1900–1909, Nov. 2013.
[44] Z. Wang and R. Paranjape, "A signal processing application for evaluating self-monitoring blood glucose strategies in a software agent model," *Comput. Methods Prog. Biomed.*, vol. 120, no. 2, pp. 77–87, Jul. 2015.
[45] C. Gibbs, *TEEMA Reference Guide, Version 1.0*. Regina, SK, Canada, TRlabs, 2000.
[46] *Power Generation in Canada*. Can. Electr. Assoc., Ottawa, ON, Canada, 2006.
[47] S. Boyd and L. Vandenberghe, *Convex Optimization.* Cambridge. U.K.: Cambridge Univ. Press, 2004.
[48] I. Richardson and M. Thomson. (Feb. 20, 2010). *Domestic Electricity Demand Model—Simulation example*. [Online]. Available: https://dspace.lboro.ac.uk/2134/5786
[49] I. Richardson, M. Thomson, D. Infield, and C. Clifford, "Domestic electricity use: A high-resolution energy demand model," *Energy Build.*, vol. 42, no. 10, pp. 1878–1887, Oct. 2010.
[50] Z. Wang and R. Paranjape, "An evaluation of electric vehicle penetration under demand response in a multi-agent based simulation," in *Proc. IEEE Elect. Power Energy Conf.*, Calgary, AB, Canada, Nov. 2014, pp. 1–6.
[51] Z. Wang and R. Paranjape, "Optimal scheduling algorithm for charging electric vehicle in a residential sector under demand response," in *Proc. IEEE Elect. Power Energy Conf.*, London, ON, Canada, pp. 1–5.
[52] K. Young, C. Wang, L. Y. Wang, and K. Strunz, "Electric vehicle battery technologies," in *Electric Vehicle Integration into Modern Power Networks* (Power Electronics and Power Systems). New York, NY, USA: Springer, 2013, pp. 15–56.
[53] C. Madrid, J. Argueta, and J. Smith, *Performance Characterization—1999 Nissan Altra-EV With Lithium-ion Battery*. Rosemead, CA, USA: Southern California EDISON, Sep. 1999.
[54] M. Grant and S. Boyd. (Sep. 2013). *CVX: MATLAB Software for Disciplined Convex Programming, Version 2.0 beta*. [Online]. Available: http://cvxr.com/cvx
[55] M. Grant and S. Boyd, "Graph implementations for nonsmooth convex programs," in *Recent Advances in Learning and Control* (Lecture Notes in Control and Information Sciences), vol. 371, V. Blondel, S. Boyd, and H. Kimura, Eds. Berlin, Germany: Springer-Verlag, 2008, pp. 95–110. [Online]. Available: http://stanford.edu/~boyd/graph_dcp.html

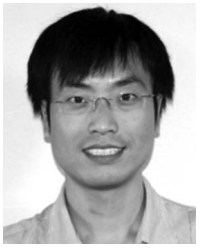

Zhanle Wang (S'12) received the B.Eng. degree in industrial automation from the North China University of Science and Technology, Langfang, China, in 2001, and the M.A.S. degree in electronic systems engineering from the University of Regina, Regina, SK, Canada, in 2012, where he is currently pursuing the Ph.D. degree.

From 2001 to 2010, he was a Staff Member and the Section Head with the Department of Academic Affairs, North China University of Science and Technology, Langfang, China. His current research interests include computational methods for power system and smart grid, including demand response optimization, optimal dispatch of power generation, and renewable energy integration.

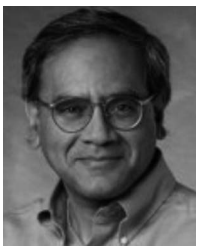

Raman Paranjape (S'81–M'90) received the B.S., M.S., and Ph.D. degrees in electrical engineering from the University of Alberta, Edmonton, AB, Canada, in 1981, 1984, and 1989, respectively.

From 1990 to 1992, he was a Research Associate with the University of Calgary, Calgary, AB. In 1992, he joined Array Systems Computing Inc., North York, ON, Canada, as a Research Scientist and the Project Manager. Since 1997, he has been with the Faculty of Engineering and Applied Science, University of Regina, Regina, SK, Canada, where he became a Full Professor in 2004. He has published over 150 journal and conference papers. His current research interests include mobile agents systems, ultrasonic visualization and nondestructive testing, robotic sensor systems, and signal and image processing.

Dr. Paranjape was a co-recipient of the Association of Professional Engineers and Geoscientists of Saskatchewan Exceptional Engineering Project Award in 2010. He was the General Chair of the IEEE Canadian Conference on Electrical and Computer Engineering, Regina, in 2013. He has been the Chair of the IEEE South Saskatchewan Section (01–02, 03–06, 11–13) and he is currently serving as the National Secretary of IEEE Canada.